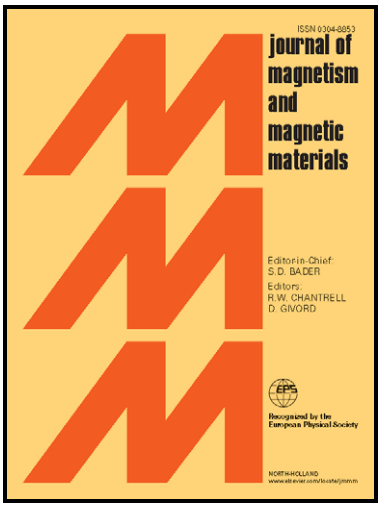

Low carbon steel samples deformed by cold rolling – analysis by the magnetic adaptive testing

Ivan Tomáš, Gábor Vértesy, Satoru Kobayashi, Jana Kadlecová, Oleksandr Stupakov

PII: S0304-8853(09)00323-0
DOI: doi:10.1016/j.jmmm.2009.03.061
Reference: MAGMA 55414

To appear in: *Journal of Magnetism and Magnetic Materials*

Received date: 24 June 2008
Revised date: 29 January 2009

Cite this article as: Ivan Tomáš, Gábor Vértesy, Satoru Kobayashi, Jana Kadlecová and Oleksandr Stupakov, Low carbon steel samples deformed by cold rolling – analysis by the magnetic adaptive testing, *Journal of Magnetism and Magnetic Materials* (2009), doi:10.1016/j.jmmm.2009.03.061

Low Carbon Steel Samples Deformed by Cold Rolling – Analysis by the Magnetic Adaptive Testing

by

Ivan Tomáš[a*], Gábor Vértesy[b], Satoru Kobayashi[c], Jana Kadlecová[a], and Oleksandr Stupakov[a**]

[a]*Institute of Physics, ASCS, Prague, Czech Republic*
[b]*Research Institute for Technical Physics and Materials Science, Budapest, Hungary*
[c]*NDE and Science Research Center, Iwate University, Morioka, Japan*

Abstract

Three series of samples of low carbon steel were investigated by the method of Magnetic Adaptive Testing (MAT). The samples were plastically deformed by cold rolling to five consecutive stages of deformation. Samples in one series were magnetically closed, those in the other two series were magnetically open. The presented results of MAT – typical by its low required magnetization of the samples – show highly sensitive and reliable correlation with plastic deformation and as a consequence also with mechanical embrittlement of the investigated material, regardless of the sample shape.

PACS: 75.50.Bb; 81.70.Ex; 75.60.Ej

Keywords: Magnetic NDE, Magnetic Adaptive Testing, Plastic deformation, Embrittlement, Low carbon steel

* Corresponding author. Tel.: +420 721 873 360; fax: +420 286 890 527
E-mail address: tomas@fzu.cz
** *presently on leave at the Institute of Fluid Science, Tohoku University, Sendai, Japan*

1. Introduction

Presence of defects and generally any variation of structure of ferromagnetic materials are reflected by details of their magnetization processes, e.g. by shape modifications of hysteresis loops, when the materials are magnetized by applied fields. Classical parameters of major hysteresis loops, such as coercive field, H_C, remanent magnetic induction, B_R, maximum permeability, μ_{MAX}, and several others, are traditionally used for nondestructive indication of the ferromagnetic construction materials degradation since long time, and a number of corresponding techniques were successfully industrially applied, see e.g. [1–6]. The traditional use of the major hysteresis loops parameters requires magnetic saturation of the tested objects, which is often not very easy to achieve. Also, the classical major loop parameters were actually defined and introduced for other purposes than the magnetic description of the non-magnetic modifications of the materials, and are not optimized for the purpose.

An alternative method, based on magnetic *minor* loops measurement was considered recently [7], and it proved to be not only experimentally *more friendly* (not requiring the magnetic saturation), but it showed to be even substantially *more sensitive* in any of the so far tested cases. The method of Magnetic Adaptive Testing (MAT) introduced general magnetic descriptors to diverse variations in non-magnetic properties of ferromagnetic materials, the descriptors *optimally adapted* to the just investigated property and the material.

The present paper describes analysis of investigation of three series of low-carbon cold-rolled steel samples, as they were studied by the method of Magnetic Adaptive Testing (MAT) in the Institute of Physics, Prague, and in the Research Institute for Technical Physics and Materials Science, Budapest, lately. Short summary of the main features of the MAT investigation was briefly discussed at the SMM18 conference [8] and at the Far East Forum for NDE [9], highlighting primarily the fact, that even though MAT-measurement on magnetically open and magnetically closed samples proceeds by different approaches, the resulting curves are qualitatively the same in both cases. The present paper intends to show details of the MAT evaluation, together with variety of the parameters available for description of plastic deformation stages of this ferromagnetic material, as it is offered by the multi-parametric method of MAT.

The samples were produced by Prof. S. Takahashi and his co-workers from the Non Destructive Evaluation and Science Research Center (NDESRC) at the Iwate University in Morioka, Japan, and made available as round robin samples for successive international measurements by laboratories gathered in the Universal Network for Magnetic Non-Destructive Evaluation (UNMNDE), see e.g. [10] for more detailed information. Takahashi et al. studied the samples mechanical properties, and related them to magnetic NDE parameters obtained from a special analysis [11] of minor hysteresis loops measured on magnetically closed picture-frame shapes of the material [12].

Section 2 of this paper reviews information about the investigated material and ways of processing the samples before measurement, as was this information made available by the producers. Section 3 reminds basic features of the presently applied method of magnetic investigation, MAT. Section 4 is devoted to description of main results as they were obtained on samples of three different shapes, namely on magnetically closed picture-frames, and on magnetically open bars and plates. Discussion of the results and of the MAT-method is given in Section 5, whereas the main conclusions are summarized in Section 6.

2. Material and samples

The material of all the samples is low-carbon steel with the chemical composition of C (0.16 w%), Si (0.20 w%), Mn (0.44 w%), and the rest of Fe. Convenient pieces of the material were cold-rolled down to plastic deformation, $\varepsilon = 0$, 5, 10, 20 and 40%, and then the samples of desired dimensions and shapes were carefully machined from the deformed steel. Three series of different

shapes, each series having five samples of progressively increasing ε-values, were prepared: the picture-frames (samples Af1 – Af5) had thickness 10mm and the external and internal dimensions 25x9mm and 20x4mm, respectively; the rectangular plates (samples Ap1 – Ap5) had dimensions 60x40x10mm; and the rectangular bars (samples Ab1 – Ab5) had dimensions 55x10x10mm. The samples were machined in such a way, that direction of the preceding cold rolling agreed with the longest dimension of each of the samples. Sketch of all the samples can be seen in Fig.1. The frame samples were equipped with a magnetizing coil (220 turns) and a pick-up coil (180 turns) each. At one side of the bar samples a V-shaped notch was machined, so that the same samples could also be used for Charpy mechanical tests. Detailed mechanical properties of the samples – Vickers hardness (VH), ductile-brittle transition temperature (DBTT), density of dislocations, and TEM micrographs – together with their magnetic reflections by Takahashi's analysis of the minor loops and by MAT can be found in [12] and [13], respectively.

Fig. 1. Dimensions and shapes of the frame-, plate- and bar-samples.

3. Magnetic Adaptive Testing

The non-destructive method of Magnetic Adaptive Testing was developed [7], and successfully assessed for a number of ferromagnetic materials and modifications of their properties [14-17]. MAT originated as an expansion of traditional magnetic hysteresis tests. In contrast to the traditional hysteresis methods, where every sample is characterized by its *single major* hysteresis loop, MAT investigates a complex *set of minor* hysteresis loops for each sample of the measured series. Every measured set of minor hysteresis loops is then re-computed into a matrix of elements. Each element of the matrix can be used as a magnetic descriptor of the material degradation. Each element is positioned by a couple of field coordinates (*F, A*), where *A* is amplitude of the minor loop in question and *F* is the field-position of the matrix element on the loop. Any succession of matrix elements with the same coordinates, of all the samples, ordered according to the increasing material degradation is called a *MAT-degradation-function*. Degradation functions with different coordinates react differently to the investigated degradation and MAT uses a procedure, which is able to pick up those, which react optimally to the considered way of degradation of the studied material. The optimal, the most sensitive and the most reliable descriptors are then used for testing of the structural modifications of the material in question.

If the samples are magnetically closed thin rings and the current in the magnetizing coil is varied in a triangular way (as a rule with the amplitude of the triangles gradually increasing by a pre-defined step), then the signal induced in the pick-up coil is proportional to differential permeability, μ, of the sample material. The recorded signal from each sample is then re-computed into the *permeability matrix* $\mu(F, A)$. The inside-sample field-coordinates are easily calculated from the corresponding values of the magnetizing current, I_F and I_A as

$$A=I_A*N/L \quad \text{and} \quad F=I_F*N/L \tag{1}$$

with N being number of turns of the magnetizing coil and L the circumferential length of the ring sample. It is advisable to keep absolute value of the time-slope of all the current triangles the same and preferably low.

In case of other sample shapes, with magnetically open samples in particular, the picked up signal is not exactly proportional to differential permeability and mostly it is not easy to re-calculate values of the magnetizing current to the acting field values. As the general shape of the signal recorded on open samples does not differ from the shape of the differential permeability on closed samples qualitatively, however, the primary voltage signal from the pick-up coil is routinely also called the "permeability" μ-signal (actually it is the average differential permeability of the whole non-uniform

magnetic circuit created by the magnetizing yoke together with the sample) and the respective matrices of the material-degradation descriptors are also routinely referred to as permeability matrices, $\mu(I_F, I_A)$. However, as calculation of the field magnitudes inside the open samples is difficult, either just the magnetizing current coordinates, I_A and I_F, of the descriptors are used or it is necessary to measure the magnetizing field values directly, separated from the measured signal in the pick-up coil (see e.g. [18,19]).

4. Results

Picture-frame samples, Af1 – Af5

Two measurements, assessed at two different Permeameters (P1 and P2), of the picture-frame samples, Af1 – Af5, are presented in Fig.2. The principal difference between the measurements was the applied rate of change of the magnetizing current. This was 186 mA/s (i.e. the calculated 704 A/m/s magnetizing field rate of change) used with Permeameter P1, and 970 mA/s (i.e. the calculated 3678 A/m/s magnetizing field rate of change) used with P2 at the top row of plots and the bottom row of plots in Fig.2, respectively. Beside this more than five times difference in the applied magnetizing speed, the measurement at P2 is also characterized by *substantially larger signal-to-noise ratio* than at P1, given by inherent properties of the two applied measuring set-ups.

The left plots in each of the rows (Fig.2 *a1* and Fig.2 *a2*) depict the signals, as they were directly recorded from the pick-up coils during the triangular variation of current in the magnetizing coils. The signal is proportional to values of the differential permeability, $\mu(I_F, I_A)$. Note the different vertical scales of these two plots.

The middle plots (Fig.2 *b1* and Fig.2 *b2*) present sensitivity maps of degradation functions computed from the signal – actually they are sensitivity maps of the *reciprocal* signal, i.e. proportional to the reciprocal differential permeability, $1/\mu$. Each sensitivity map illustrates relative sensitivity of $1/\mu(F_i, A_j, \varepsilon)$*-degradation functions,* computed as the slope of the linear fit to each of the degradation function. The dark color at field-coordinates (F_i, A_j) means low sensitivity of the degradation functions. The lighter the color at the coordinates, the higher sensitivity of the respective degradation function. Sensitivity of the degradation functions with coordinates $F \approx 200$ A/m, $A \geq 200$ A/m (the white vertical band) is the highest, both in Fig.2 *b1* and in Fig.2 *b2*. The plots Fig.2 *b1* and Fig.2 *b2* do not have the same scale of the sensitivity; just black is the lowest and white is the highest in each map.

The right hand side plots (Fig.2 *c1* and Fig.2 *c2*) show graphs of several degradation functions chosen from the most sensitive areas of the sensitivity maps. All the degradation functions start at unity, as the sample with zero rolling reduction (Af1) was chosen to be the normalizing reference one.

Fig.2 Series of picture-frame samples, Af1 – Af5: (*a*) measured signal, (*b*) sensitivity map of $1/\mu$-degradation functions, (*c*) $1/\mu$-degradation functions (reciprocal) chosen from the most sensitive area (the dotted $\mu(F200A250)$-degradation function (direct) is shown for comparison). Legend in the (*c*)-graphs gives the field-coordinates (in A/m). The top row of plots presents the measurement at Permeameter P1 with *lower* rate of change of the magnetizing field, the bottom row of plots corresponds to the measurement at Permeameter P2 with *five time higher magnetizing speed*.

Plate samples, Ap1 – Ap5

The plate-shaped samples, Ap1 – Ap5, were measured with the aid of a measuring yoke. The yoke used in the measurement presented in Fig.3 was a U-shaped core made of laminated silicon-iron sheets, with N=136 turns of the magnetizing coil wound on the bow of the yoke, and with n=50 turns of the pick-up coil wound on one of the yoke legs. Lateral dimensions of the measuring yoke can be characterized by its cross-section: S=25.8x9.9mm^2, the total outside length 36.9mm, and the total outside height of the bow 36.5mm. The measurement was performed at Permeameter P1, the rate of change of the magnetizing current was 942 mA/s. The samples were magnetized along the shorter side of the plate, i.e. perpendicular to the direction of the rolling.

Three pairs of graphs are presented in two rows of plots in Fig.3. The top row is similar to any of the rows of Fig.2. Namely the far left graph (Fig.3 *a1*) presents the voltage signal directly measured from the pick-up coil during the triangular variation of the magnetizing current. The middle plot (Fig.3 *b1*) of the first row is the sensitivity map of the *reciprocal* signal, i.e. of the $1/\mu(I_{Fi}, I_{Aj}, \varepsilon)$-degradation functions. The far right graph (Fig.3 *c1*) shows several typical $1/\mu(I_{Fi}, I_{Aj}, \varepsilon)$-degradation functions chosen from the most sensitive area of the $1/\mu$-sensitivity map, with the legend giving their current-coordinates (I_{Fi}, I_{Aj}) in mA. Note that results of the measurement of magnetically open samples with the measuring yoke are parametrized by the magnetizing *current* values.

The bottom row of graphs in Fig.3 starts with the plot (Fig.3 *a2*) of the same voltage signal as in Fig.3 *a1*, showing details in the first quadrant only, however. The middle plot (Fig.3 *b2*) of the second row is the sensitivity map of the *direct* signal, i.e. of the $\mu(I_{Fi}, I_{Aj}, \varepsilon)$-degradation functions. The far right graph (Fig.3 *c2*) shows several typical $\mu(I_{Fi}, I_{Aj}, \varepsilon)$-degradation functions chosen from the most sensitive area of the μ-sensitivity map, with the legend giving their current-coordinates (I_{Fi}, I_{Aj}) in mA.

It is worth of mentioning that the measured signal (see graph Fig.3 *a1* and the same in detail in Fig.3 *a2*) reveals its two usable areas. Namely that around the magnetizing current values $0<I_F<200$ mA, and/or that around the magnetizing current values $400<I_F<700$ mA, where magnitudes of the signals proceed in the reversed order and/or in the same order as the values of the rolling reduction, ε, of the samples, respectively. The $1/\mu$-sensitivity map in the plot Fig.3 *b1* shows the white area of the (I_{Fi}, I_{Aj})-coordinates of the most sensitive, *reciprocal*, $1/\mu$-degradation functions, and the plot Fig.3 *c1* presents several examples of them. The μ-sensitivity map in the plot Fig.3 *b2* shows the white area of the (I_{Fi}, I_{Aj})-coordinates of the most sensitive, *direct*, μ-degradation functions, and the plot Fig.3 *c2* presents examples of them.

Fig.3 Series of plate-shaped samples, Ap1 – Ap5: (*a*) measured signal, (*b*) sensitivity map of degradation functions, (*c*) degradation functions chosen from the most sensitive area. Legend in the (*c*)-graphs gives the current-coordinates (in mA). See the detailed description within the text.

Bar samples, Ab1 – Ab5

Also the bar-shaped samples, Ab1 – Ab5, were measured by a measuring yoke. Fig.4 presents results obtained by Permeameter P2 and the yoke (a similar C-shaped laminated Fe-Si transformer core), with N=200 turns of the magnetizing coil wound on the bow of the yoke, and with n=40 turns of the pick-up coil wound on one of the yoke legs. Lateral dimensions of the measuring yoke (characterized by its cross-section): S=10x8 mm^2, the total outside length 27 mm, and the total outside height of the bow 26 mm. The rate of change of the magnetizing current was 568 mA/s. The yoke was attached along the length of the bar samples, to the smooth surface at the face opposite to the V-notch.

The arrangement of Fig.4 is the same as in Fig.3: Namely the far left graph (Fig.4 *a1*) of the top row presents the voltage signal from the pick-up coil, the middle top plot (Fig.4 *b1*) is the sensitivity map of the *reciprocal* signal, i.e. of the $1/\mu(I_{Fi}, I_{Aj}, \varepsilon)$-degradation functions. The far right top graph (Fig.4 *c1*) shows several typical degradation functions chosen from the most sensitive area of the $1/\mu$-sensitivity map.

The bottom row of graphs in Fig.4 starts with the plot (Fig.4 *a2*) of the same voltage signal as in Fig.4 *a1*, showing details of the first quadrant only. The middle bottom plot (Fig.4 *b2*) is the sensitivity map of the *direct* signal, i.e. of the $\mu(I_{Fi}, I_{Aj}, \varepsilon)$-degradation functions. The far right bottom graph (Fig.4 *c2*) shows typical μ-degradation functions chosen from the most sensitive area of the μ-sensitivity map, with the legend giving their current-coordinates (I_{Fi}, I_{Aj}) in mA.

The measured signal (see graph Fig.4 *a1* and the same in detail in Fig.4 *a2*) reveals its two usable areas. Namely that around the magnetizing current values $-50<I_F<100$ mA, and/or that around the magnetizing current values $150<I_F<300$ mA, where magnitudes of the signals proceed in the reversed order and/or in the same order as the values of the rolling reduction of the samples, respectively. The $1/\mu$-sensitivity map in the plot Fig.4 *b1* shows the white area of the (I_{Fi}, I_{Aj})-coordinates of the most sensitive, *reciprocal*, $1/\mu$-degradation functions, and the plot Fig.4 *c1* presents examples of them. The μ-sensitivity map in the plot Fig.4 *b2* shows the white area of the (I_{Fi}, I_{Aj})-coordinates of the most sensitive, *direct*, μ-degradation functions, and the plot Fig.4 *c2* presents examples of them.

Fig.4 Series of bar-shaped samples, Ab1 – Ab5: (*a*) measured signal, (*b*) sensitivity map of degradation functions, (*c*) degradation functions chosen from the most sensitive area. Legend in the (*c*)-graphs gives the current-coordinates (in mA). See the detailed description within the text.

5. Discussion

It is an inherent property of MAT – as of any multi-parametric testing of material variation – that the final choice of the descriptors of the investigated changes depends on the experimenter's opinion about what is the optimum result for the investigation in question. This fact is the more emphasized in the present paper, where the low carbon steel material is degraded in the same way, but it is investigated on samples of several shapes and measured by several attitudes. Generally, the basic difference between the attitudes is observed if magnetically closed and magnetically open samples are used.

Magnetically closed samples are the most convenient from the point of view of MAT. The closed samples make a uniform magnetic circuit, no fluctuation of any magnetic contact makes problem, minimum stray field escapes from the coils wound directly on the sample body, the magnetizing field inside the sample material can be easily calculated from the magnetizing current and field coordinates of the convenient degradation functions unambiguously characterize their positions. Our closed samples, Af1 – Af5, were thin picture-frames and the inside-sample fields were similar to those, given by the simple calculation (1). Results of the MAT measurement presented in Fig.2 show a continuous area of the sensitive $1/\mu$-degradation functions, starting at minor loop amplitudes far before the saturation amplitude (see Fig.2 *b1 b2*), with sensitivity almost independent on the amplitude value (see Fig.2 *c1 c2*). The most sensitive area is situated at the magnetizing field values corresponding closely to the top permeability magnitudes of the softest sample Af1 (see Fig.2 *a1 a2* and Fig.2 *b1 b2* using the coefficient N/L=3793m^{-1}). Drop of the *direct* μ-values in this area of the field coordinates, from "1" of the normalizing sample Af1 down to *smaller*, positive μ-values (see the black dots in Fig.2 *c1*) for the other samples material (compressed more and more by the rolling), makes the reason why use of the *reciprocal* $1/\mu$-degradation functions, which smoothly increase from "1" to *large* positive values, is more convenient.

Comparison of the "slow" measurement by Permeameter P1 in the top row of plots in Fig.2, with the five times faster measurement by P2 in the bottom row, illustrates the ease of increasing the measured signal if needed (as here for instance for obtaining a better signal-to-noise ratio). However, application of a faster rate of change of the magnetizing field is often paid for by getting lower sensitivity of the corresponding degradation functions (compare Fig.2 *c1* and Fig.2 *c2*), see also [20] for general analysis of the matter.

MAT measurement of the magnetically open plate-samples (Ap1 – Ap5) and bar-samples (Ab1 – Ab5) had to be carried out with the aid of measuring yokes. Even though the MAT results agree with each other (compare Fig.3 with Fig.4), and also with measurements on magnetically closed samples (compare with Fig.2) qualitatively, they differ quantitatively, see also [9]. This means, that any application of Magnetic Adaptive Testing requires the measurements to be always carried out under *the same experimental conditions*. For the measurement to be quantitatively comparable, it is necessary to apply *the same rate of change of magnetization*, *the same shape of samples, and the same measuring yoke* (in case of open samples).

An experimental condition to be discussed separately is the *quality of magnetic contact* between the measuring yoke and the sample surface. This, of course, is also strictly *required to be the same* at each of the measurement, as otherwise the uncontrolled fluctuation of the magnetic contact varies the relation between magnitude of the magnetizing current and magnitude of the inside-sample-field arbitrarily, and the current-coordinates of degradation functions are then useless. In case the magnetic contact cannot be kept the same, then the only way how to secure repeatability and reliability of the quantitative MAT testing, is to find out the magnetizing-*field*-coordinates even at the open samples, namely by an independent determination of the inside-sample field. This is possible by

extrapolation of the tangential field independently measured at the surface of the samples (for analysis of the problem see e.g. [18,19]).

Some variability of the experimental conditions, including limited fluctuation of the magnetic contact, can be tolerated, however, if the useful degradation functions are picked-up from a convenient area of the sensitivity map. Such convenient areas are the "vertical" white bands, which can be seen in all the sensitivity maps presented in this paper. Examine for instance white band in the μ-sensitivity map of Fig.3 *b2*. The degradation functions μ-(I_F=600A/m, I_A≥750A/m, ε) do not depend on the minor loop amplitude (see Fig.3 *c2*), and their field coordinate I_F=600A/m can be independently pinpointed as a local maximum of normalized signal minor loops with any amplitude I_A≥750A/m. Magnetic conditions of the degraded samples within these amplitude limits give birth to the *identical degradation functions*. Moreover, as can be seen in [20], sensitivity of degradation functions from *some* areas of the sensitivity map is practically independent on the applied rate of change of the sample magnetization. This makes such MAT evaluation of the material degradation highly robust and tolerant with respect to some degree of fluctuation of the measuring conditions.

As seen from Fig.3 and Fig.4, MAT measurement on both the plate and the bar samples allowed determination of not only the reciprocal degradation functions sensitive areas – Fig.3 *b1* and Fig.4 *b1* – close to the top μ-magnitude of the magnetically softest samples (similar to that area in Fig.2 *b1* and/or Fig.2 *b2* at the frame samples) but it showed one more sensitive area of the degradation functions, this time of the *direct* μ-degradation functions around the "tail" values of the signal. Figures 3 *a1*, 4 *a1*, and in particular the detailed Fig.3 *a2*, Fig.4 *a2* reveal that the magnitudes of the μ-signals are in those "tail" areas ordered directly along with the rolling reduction values of the samples. Fig.3 *b2* and Fig.4 *b2* show high sensitivity of those direct degradation functions within the μ-sensitivity maps and Fig.3 *c2* and Fig.4 *c2* give examples of the direct μ-degradation functions from those areas. As shown in [20], sensitivity of degradation functions derived from the "tail" values of the signal is almost independent on the rate of change of the sample magnetization.

A range of corresponding direct μ-degradation functions was *not* discovered at the frame samples testing. Partial tendency toward such behavior appeared, but no completely monotonous, increasing, μ-degradation function was found for the frame samples series. This, together with details of shapes of the degradation functions for the presented individual measurements, supports the imperative that best reliable comparison of the MAT measurements is achieved by as close repetition of the experimental conditions as possible.

In cases of smooth MAT measurements, as for instance at the series of the magnetically closed frame-samples, it seems expedient to construct also data matrices of the first derivative of permeability $\mu' = \mathrm{d}\mu/\mathrm{d}F$ and/or of its reciprocal values. The $1/\mu'$-sensitivity map, computed from the $1/\mu'$-data matrices is shown in Fig.5 together with some representative $1/\mu'$-degradation functions taken from the area of top sensitivity. As can be seen, stability of determination of the top sensitive $1/\mu'$-degradation functions within the $1/\mu'$-sensitivity map is not substantially worse than position of similar $1/\mu$-degradation functions within the $1/\mu$-sensitivity map, and even the "vertical band" of independence on minor loops amplitude is present. Sensitivity of the $1/\mu'$-degradation functions exceeds that of the $1/\mu$-functions at least twice – compare plots Fig.2 *c1* and Fig.5 *c*.

Fig.5 Series of picture-frame samples, Af1 – Af5: Picture (*a*), which should correspond to the first derivative of the signal in Fig.2 *a1*, was omitted intentionally – the numerical derivative of measured signals of the five samples provides an illegible plot. Picture (*b*) is a $1/\mu'$-sensitivity map computed from the series of $1/\mu'$-data matrices. The $1/\mu'$-degradation functions taken from the area of the top sensitivity show extremely high steepness with respect to the rolling deformation of the material – see plot (*c*). Legend in the (*c*)-graph gives the field-coordinates (in A/m).

The MAT measurement on the plate samples was carried out with magnetization of the samples both along the rolling direction and perpendicular to the rolling direction. Slight systematic differences between these two directions of magnetization were observed. However, as also the lengths of the samples in those two directions differ from each other, it was not possible to evaluate any reliable systematic conclusion in this respect. Our measurement suggested that (unlike e.g. in the case of plastic deformation of such material by uniform mechanical tension) magnetic anisotropy with respect to the used rolling conditions was not substantial.

The MAT measurement on the bar samples was carried out with the measuring yokes attached both at the surface *without* the V-notch and at the surface *with* the V-notch. Very slight systematic difference in the signal values under these two configurations was observed. However, no substantial inference from this was concluded either. The MAT measurement, being an integral test of the material volume, can hardly be expected to do so.

Detailed investigation of magnetic reflection of traditional mechanical properties of the studied samples via MAT [13] reveals linear dependence of the optimum degradation functions on VH and on DBTT. Steepness of each relation depends on the way of each magnetic measurement, however, all of them are linear and all of them allow determination of VH and DBTT of the material with precision not worse than the mechanical measurements themselves.

6. Conclusions

Detailed analysis of Magnetic Adaptive Testing investigation of three series of samples of low carbon steel, prepared in the frame of a chain of magnetic non-destructive measurements on round robin samples, organized by the Universal Network for Magnetic Non-Destructive Evaluation, was described. Sample shapes, ways of measurement, signal-to-noise ratios, speed of magnetization and sensitivity and choice of degradation functions were discussed.

Application of MAT required only low magnetization of the samples, and yielded highly sensitive and reliable correlation with compressive plastic deformation of the investigated steel and – as shown in [13] – therefore also with its hardness and mechanical brittleness. The method can be successfully applied also on magnetically open samples: identical correlation between magnetic descriptors and mechanical degradation of the material was found both in the magnetically open samples, and in the magnetically closed ones. The presented results produce sound support to next experiments with application of MAT as a *magnetic, nondestructive, low magnetization requiring, complementary method* to the mechanical *destructive* tests within surveillance programs of nuclear pressure vessels steel embrittlement.

Acknowledgements

The authors are obliged to the Universal Network for Magnetic Non-Destructive Evaluation for organization of the round robin samples preparation and measurements, the presented paper being just one contribution to the complex view of the used materials. The authors are also thankful for the financial support under projects No.1QS100100508 and No.102/06/0866 of the Academy of Sciences and of the Grant Agency of the Czech Republic, by Hungarian Scientific Research Fund (project K-

62466) and by the Czech-Hungarian Bilateral Intergovernmental S&T Cooperation. O.Stupakov appreciates the financial support by JSPS postdoctoral fellowship.

References

[1] M.J.Johnson, C.C.H.Lo, B.Zhu, H.Cao, D.C.Jiles, J. Nondestruct. Eval. **20** (2000) 11.
[2] D.C.Jiles, Magnetic methods in nondestructive testing, K.H.J.Buschow et al., Ed., Encyclopedia of Materials Science and Technology, Elsevier Press, Oxford, (2001) p.6021.
[3] I. Mészáros, Mater.Sci.Forum, **473-474** (2005) 231.
[4] H.Kronmüller, M.Fähnle, in Micromagnetism and the Microstructure of Ferromagnetic Solids, Cambridge University Press, Cambridge, 2003.
[5] D.C.Jiles, NDT Int. **21** (1988) 311.
[6] J.Blitz, Electrical and magnetic methods of nondestructive testing (Adam Hilger IOP Publishing, Ltd., Bristol, 1991).
[7] I.Tomas, J.Magn.Magn.Mater. **268** (2004) 178
[8] I.Tomas, G.Vertesy, S.Kobayashi, J.Kadlecova, O.Stupakov, Round Robin Steel Samples Deformed by Cold Rolling – Investigation by Magnetic Adaptive Testing, 18th Int.Conf.Soft Magn.Mater. (SMM18), Cardiff, UK, September 2007, unpublished
[9] G.Vertesy, I.Tomas, S.Kobayashi, Nondestructive Evaluation of Low Carbon Steel by Magnetic Adaptive Testing, 2008 Far East Forum on Nondestructive Evaluation/Testing: New Technology & Application, Nanjing, China, June 2008
[10] http://www.ndesrc.eng.iwate-u.ac.jp/UniversalNetwork/html/main.html
[11] S.Takahashi, L.Zhang, J.Phys.Soc.Japan **73** (2004) 1567
[12] S.Takahashi, S.Kobayashi, H.Kikuchi, Y.Kamada, J.Appl.Phys. **100** (2006) 113908
[13] G.Vertesy, I.Tomas, S.Takahashi, S.Kobayashi, Y.Kamada, H.Kikuchi, NDT&E Int. **41** (2008) 252
[14] I.Tomas, O.Stupakov, J.Kadlecova, O.Perevertov, J.Magn.Magn.Mater. **304** (2006) 168.
[15] G.Vertesy, T.Uchimoto, T.Takagi, I.Tomas, O.Stupakov, I.Meszaros, J.Pavo, Physica **B372** (2006) 156.
[16] G.Vertesy, I.Tomas, I.Meszaros, J.Magn.Magn.Mater. **310** (2007) 76.
[17] O.Stupakov, I.Tomas, NDT&E Int. **39** (2006) 554.
[18] O.Stupakov, I.Tomas, J.Kadlecova, J.Phys.D **39** (2006) 248.
[19] O.Stupakov, J.Magn.Magn.Mater. **307** (2006) 279.
[20] I.Tomas, G.Vertesy, J.Kadlecova, doi:10.1016/j.jmmm.2008.10.003, J.Magn.Magn.Mater. (in press),

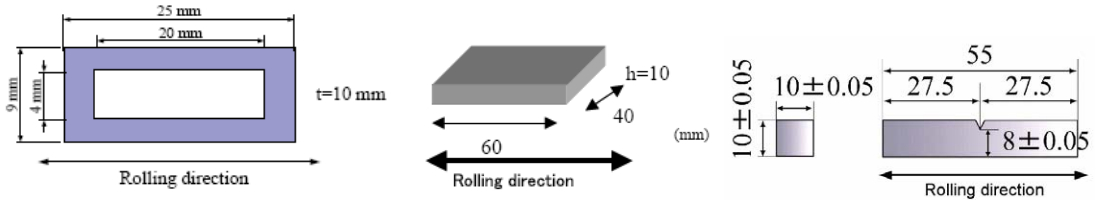

Figure 1

Figure 2:

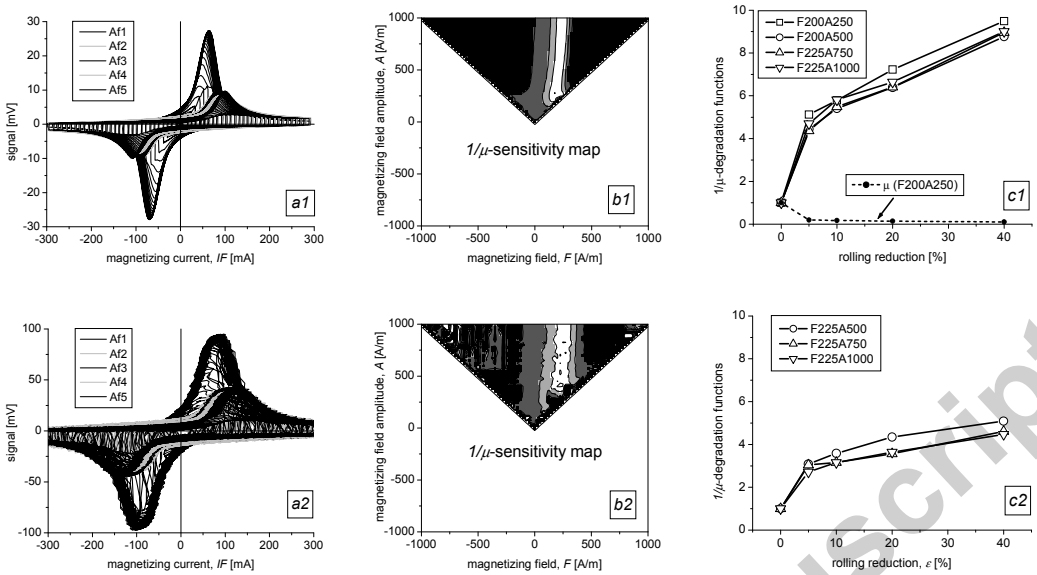

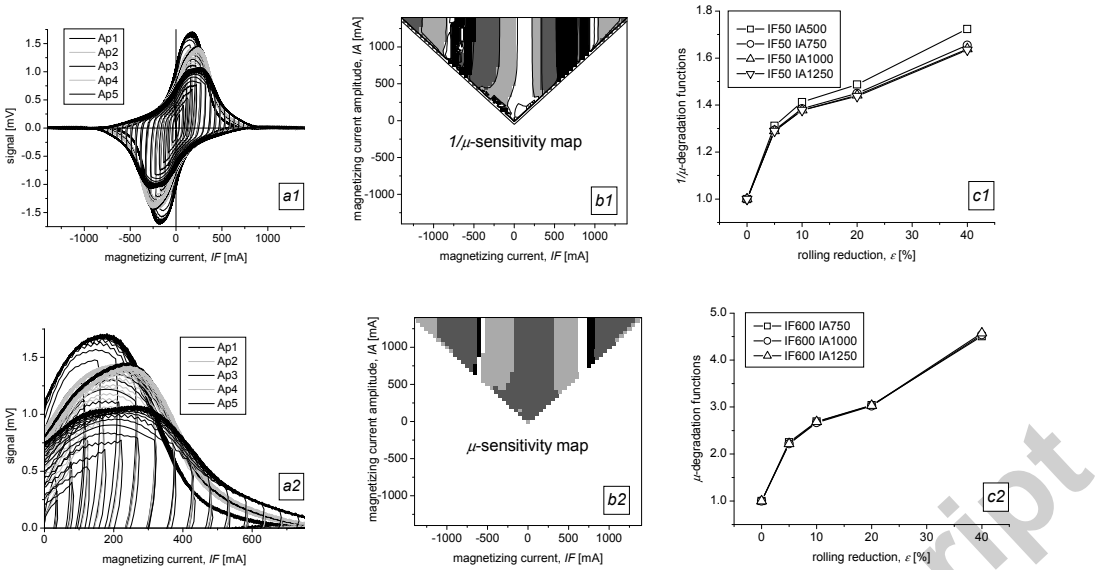

Figure 3

Figure 4:

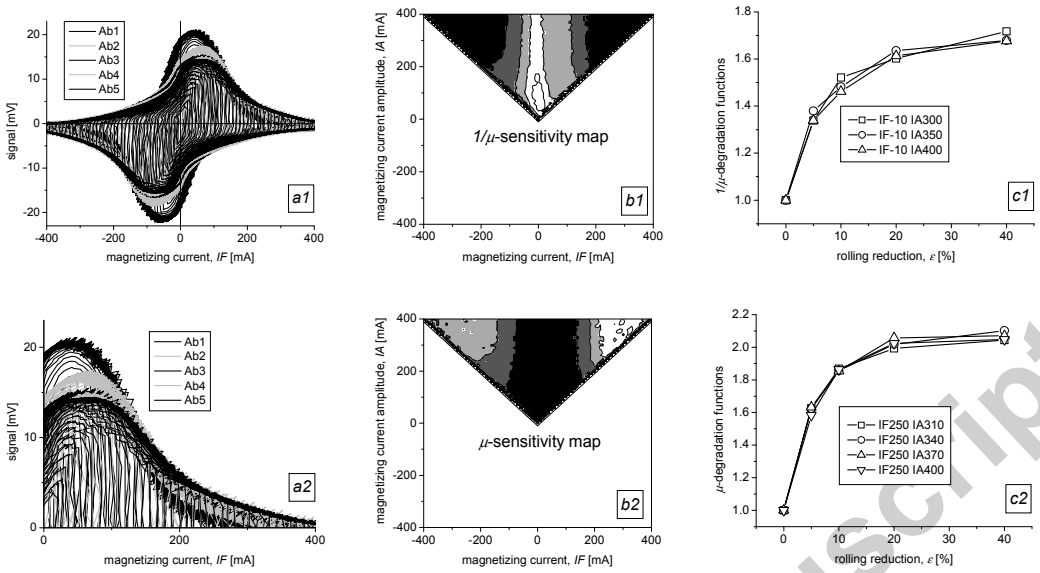

Figure 5: